

SPECIAL PROJECT PROGRESS REPORT

Progress Reports should be 2 to 10 pages in length, depending on importance of the project. All the following mandatory information needs to be provided.

Reporting year 2018.....

Project Title: Direct numerical simulation of wind wave fields in a rapidly changing environment
.....

Computer Project Account: SPGBSHRI

Principal Investigator(s): Prof V.I. Shrira

Affiliation: School of Computing and Mathematics, Keele University, Keele ST5 5BG UK

Name of ECMWF scientist(s) collaborating to the project (if applicable)

Start date of the project: 01/01/2016.....

Expected end date: 31/12/2018.....

Computer resources allocated/used for the current year and the previous one (if applicable)

Please answer for all project resources

		Previous year		Current year	
		Allocated	Used	Allocated	Used
High Performance Computing Facility	(units)	300000	300000	300000	180000
Data storage capacity	(Gbytes)	100	50	100	50

Summary of project objectives

(10 lines max)

This project aims at developing new models and algorithms for wind wave modelling, applicable for situations with fast changes of the environment, which are beyond the limits of applicability of the classical kinetic equation. Rapid changes of wind can lead to the increased probability of extreme wave events. The generalized kinetic equation (GKE) and direct numerical simulations (DNS) of wind wave fields, based on the Zakharov equation, allow tracing the evolution of spectra and higher-order moments of the field for many thousands of wave periods (at least an order of magnitude longer than with other DNS approaches). In this project, a direct comparison of the DNS and the GKE is performed, with the aim to understand the role of coherent processes, resolved by the DNS but completely filtered out in the statistical approach. These processes result in the difference in the timescales of the evolution of spectra, and affect higher statistical moments.

Summary of problems encountered (if any)

(20 lines max)

No particular problems encountered

.....

.....

.....

.....

.....

Summary of results of the current year (from July of previous year to June of current year)

This section should comprise 1 to 8 pages and can be replaced by a short summary plus an existing scientific report on the project

In this project, we study numerically long-term evolution of random water wave fields by direct numerical simulation algorithm based on the integrodifferential Zakharov equation. This algorithm does not depend on any statistical assumptions and allows one to simulate evolution of wave spectra and of higher statistical moments of the wave field. Since the Zakharov equation plays the role of the primitive equation of the theory of wave turbulence, we refer to this model as direct numerical simulation of spectral evolution (DNS-ZE). The DNS-ZE method allows to study long-term spectral evolution (up to $O(10^4)$ wave periods), which was previously possible only with the kinetic (Hasselmann) equation. Description of the algorithm can be found in Annenkov & Shrira (2018).

Results obtained with the DNS-ZE are compared with simulations performed with kinetic equations: the classical (Hasselmann) kinetic equation (KE), for which the standard WRT algorithm is used, and the generalised kinetic equation (gKE), derived using the same statistical closure as the KE, but without the assumption of quasi-stationarity, so that it can be used in fast changing environments. The latter algorithm has been described in Annenkov & Shrira (2016). Thus, we are able to perform a direct comparison of spectral evolution with and without the statistical closure, and to trace the evolution of higher statistical moments.

Results obtained in the final year of the project are outlined below. We focus on various aspects of wave field evolution in changing environments.

1. Evolution of higher statistical moments of wave fields in fast changing situations

In order to predict not just the average characteristics of wave fields, but also extremes, it is necessary to know the probability density function (p.d.f.) of surface elevations. The p.d.f. can be approximately reconstructed from the wave spectrum and at least two first higher-order moments of a random wave field (skewness and kurtosis, see Janssen 2014). Most theoretical studies of higher-order moments were confined to narrowband wave fields. However, real oceanic wave fields are not narrowband and always have a certain directional distribution. Recently, Annenkov & Shrira (2014) estimated higher-order moments of JONSWAP spectra in the large-time limit, using the theory developed by Janssen (2009). The important question is on the behaviour of higher moments, especially the kurtosis, during short-term evolution in transient fast-changing situations. As it is well-known, the kurtosis evolution for a wave field with one-dimensional spectrum crucially depends on the value of the BFI (Benjamin-Feir index, representing the ratio between nonlinearity and spectral bandwidth). If $BFI > 1$, then the kurtosis attains large positive values during short-term evolution. Measurements of the short-term kurtosis evolution for wave fields with spectra initially corresponding to JONSWAP form with various (although in all cases relatively narrow) directional distributions were performed by Onorato et al (2009). Numerical simulations by Toffoli et al (2010) and Xiao et al (2013), using high-order spectral method and Dysthe equation, showed good agreement with the experimental results. Annenkov & Shrira (2018) (see also report for the previous year), using these numerical and experimental results for the validation of the DNS-ZE algorithm, showed good agreement with the measured and previously simulated kurtosis evolution.

Here, in order to get a broader picture of the kurtosis evolution for various initial spectra, we perform a number of numerical experiments with the DNS-ZE algorithm. The questions addressed are (i) role of the initial directional distribution, (2) sensitivity of results obtained without wind forcing to the presence of moderate and strong wind (iii) dependence of the kurtosis evolution on the initial amplitude (iv) evolution in the presence of the second wave system with higher peak frequency and possibly different directional distribution. Details of the numerical procedure can be found in Annenkov & Shrira (2018). In what follows we concentrate on the dynamical kurtosis $C_4^{(d)}$, since the bound harmonics component of the kurtosis $C_4^{(b)}$, as well as the skewness C_3 , are nearly constant during short-term evolution (see Annenkov & Shrira 2013 for definition of higher moments of a wave field).

Annenkov & Shrira (2018) simulated the evolution of the kurtosis for two spectra of JONSWAP form with high peakedness ($\gamma = 6$) and directional distribution specified as

$$D(\theta) = \begin{cases} \frac{2}{\Omega} \cos^2\left(\frac{\pi\theta}{\Omega}\right) & \text{for } |\theta| \leq \Omega/2 \\ 0 & \text{for } |\theta| > \Omega/2 \end{cases} \quad (1)$$

where θ is the mean propagation direction and Ω is the directional spreading width. Two initial

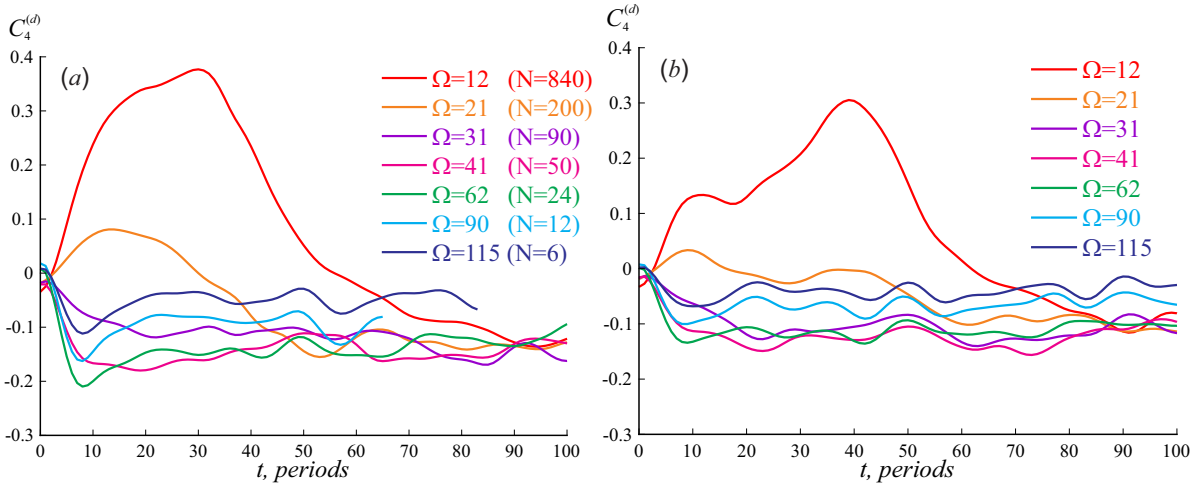


Figure 1: Evolution of the dynamical kurtosis for initial JONSWAP spectra with the significant wave height $H_s = 0.08$ m, peak period $T_p = 1$ s, and peakedness parameter (a) $\gamma = 6$ (b) $\gamma = 3$. Directional distribution is specified by (1), with different values of Ω (in degrees) corresponding to different curves. Values of N in the equivalent \cos^N directional model are also shown

values of Ω were considered, $\Omega = 12^\circ$, approximately corresponding to $N = 840$ in the frequently used \cos^N directional model, and $\Omega = 62^\circ$, which corresponds to $N = 24$ and can be considered as the typical width of swell. Here, we extend these simulations to different peakedness $\gamma = 6$ and $\gamma = 3$, and a wider range of Ω .

Figure 1 shows evolution of the dynamical kurtosis over 100 wave periods for JONSWAP spectra with $\gamma = 6$ and $\gamma = 3$, initial wave steepness 0.11, initial wave period $T_p = 1$ s and different directional distributions, ranging from almost unidirectional waves to a directionally wide spectrum typical of oceanic conditions. When the angular distribution is very narrow, the kurtosis initially evolves to high positive values, as predicted by the theory for one-dimensional wave fields. However, even for a slightly wider directional width this behaviour changes qualitatively, and for wave fields of intermediate angular width the kurtosis becomes negative during the initial evolution. For directionally wide wave fields the kurtosis still evolves towards negative values, but remains close to zero.

In Figure 2, results of the same numerical experiments are compared with those obtained in the presence of wind forcing. For the first dozen wave periods, the kurtosis evolution is unaffected by the wind, but then, due to the increased speed of the angular broadening under wind forcing, the dynamical kurtosis quickly becomes negative, approaching -0.3 for all initial spectra.

Figure 3 shows the effect of different initial amplitudes on the kurtosis evolution, for nearly one-dimensional spectrum ($\Omega = 12$) in figure 3a and intermediate angular width ($\Omega = 62$) in figure 3b. In the first case, the decrease of amplitude paradoxically leads to the increase of the kurtosis. Yet again, here we see the importance of the angular width for the kurtosis evolution. Although smaller initial amplitudes lead to weaker nonlinearity and decrease kurtosis maxima, slower angular broadening in those case gives the opposite effect in figure 3a. For intermediate

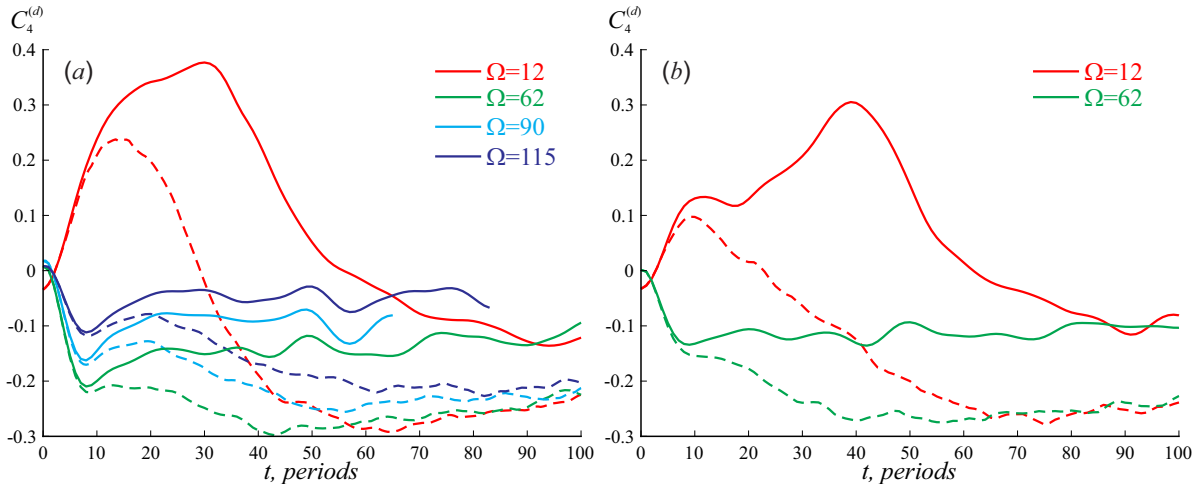


Figure 2: Evolution of the dynamical kurtosis with and without wind forcing. Initial conditions are the same as in the case of the evolution shown in figure 1*a,b*, with (a) $\gamma = 6$, (b) $\gamma = 3$. Solid curves show evolution without wind forcing, as in figure 1. Dashed curves correspond to wind forcing, with wind speed $U/c_p = 5$, where c_p is the phase velocity of the initial spectral peak

angular width, as in figure 3*b*, a decrease of amplitude decreases the absolute values of the kurtosis, as it is expected.

In figure 4, we consider the kurtosis evolution of a wave field with two spectral peaks, consisting of two superposed JONSWAP spectra. Higher-frequency spectrum has peak frequency 1.5 times higher and wider angular width, the total nonlinearity of the system being the same as in previous numerical experiments. Evolution of such wave fields shows complex kurtosis behaviour. However, it is negative in all simulations and can become rather large in absolute value, provided that the spectral width of higher-frequency waves is intermediate. The case with $\Omega_1 = \Omega_2 = 62$ is shown in figure 5 in more detail, for different relations between the peak frequencies and the same total nonlinearity of the wave field. Negative values of the kurtosis attained during evolution are maximal if the spectral peak of higher frequency spectrum is at 1.5–1.75 ω_p .

Overall, numerical simulations of the kurtosis evolution largely confirm the established picture of the kurtosis evolution, which is based on two key points (i) for a one-dimensional, or nearly one-dimensional spectrum, the dynamical kurtosis can be large provided that the spectrum is sufficiently narrow (ii) for directionally wide wave fields, typical of real oceanic conditions, the dynamical kurtosis is small and can be neglected. However, this picture is substantially enriched. First, for initially one-dimensional spectra the established behaviour of the kurtosis can be considerably affected by any factor that can enhance the rate of angular broadening (large amplitude, wind forcing, presence of another wave system in higher frequencies, etc). Second, it was found that wave fields of intermediate directional width (say, close to that of oceanic swell) show a qualitatively different behaviour, with negative dynamical kurtosis that can be moderately large in absolute value (say, -0.3–0.4 for wave steepness $O(0.1)$). Evolution of wave fields with two-peaked spectra can also lead to considerably large negative dynamical kurtosis.

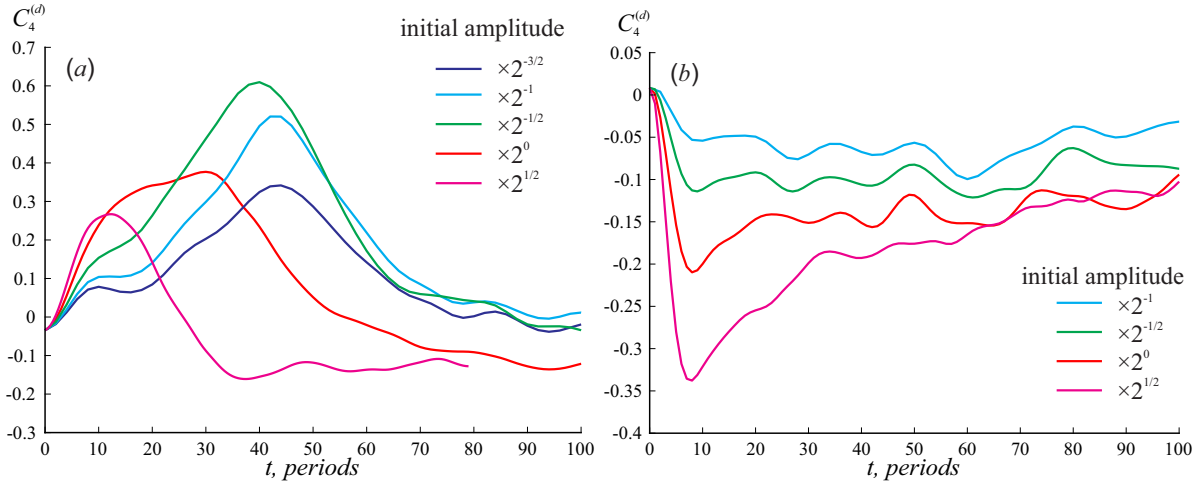


Figure 3: Evolution of the dynamical kurtosis for wave fields of different initial amplitude. Initial conditions are as in figure 1a with $\gamma = 6$ and (a) $\Omega = 12$, (b) $\Omega = 62$, with amplitudes multiplied by 2^n , where n ranges from $-3/2$ to $1/2$

2. Scaling of growth rates of wind wave spectra

Annenkov & Shrira (2018) showed that in the absence of wind forcing, spectral growth rates obtained by direct numerical simulation are characterised by dynamical, rather than statistical scaling. Thus, absolute growth rates scale with the fourth power of nonlinearity, rather than the sixth power as predicted by the Hasselmann equation (which is an equation in real variables with the prescribed scaling). Growth rates normalised by spectral amplitudes correspond to second and fourth power of nonlinearity respectively.

In this project, we perform a comparison of the growth rates obtained by DNS-ZE, KE and gKE for wind waves evolving under constant and changing wind forcing. In the former case, wind (in a number of numerical experiments, taken in the range $2 < U/c_p < 7.5$, where U is wind speed and c_p is the initial phase speed of the spectral peak) is kept constant during the evolution. In the latter case, wind forcing is instantly increased by 50% at a certain point during the evolution. In order to understand how the spectral growth rates scale with wind speed U , we find, for each wavenumber, the maximum value of $dS(k)/dt$, where $S(k)$ is the omnidirectional energy spectrum, and perform a numerical fit

$$\log \max \frac{dS(k)}{dt} = \nu \log U + \beta$$

over different values of U . Results are compared with measurements carried out in the large Marseille-Luminy wind-wave facility.

Figure 6 shows growth rate scaling obtained for constant and changing wind forcing. For constant wind, both kinetic equations give the expected statistical scaling of growth rates, in a sharp contrast with DNS-ZE and the experiment. For increasing wind, the discrepancy is found again, but the gKE demonstrates growth rates close to the DNS.

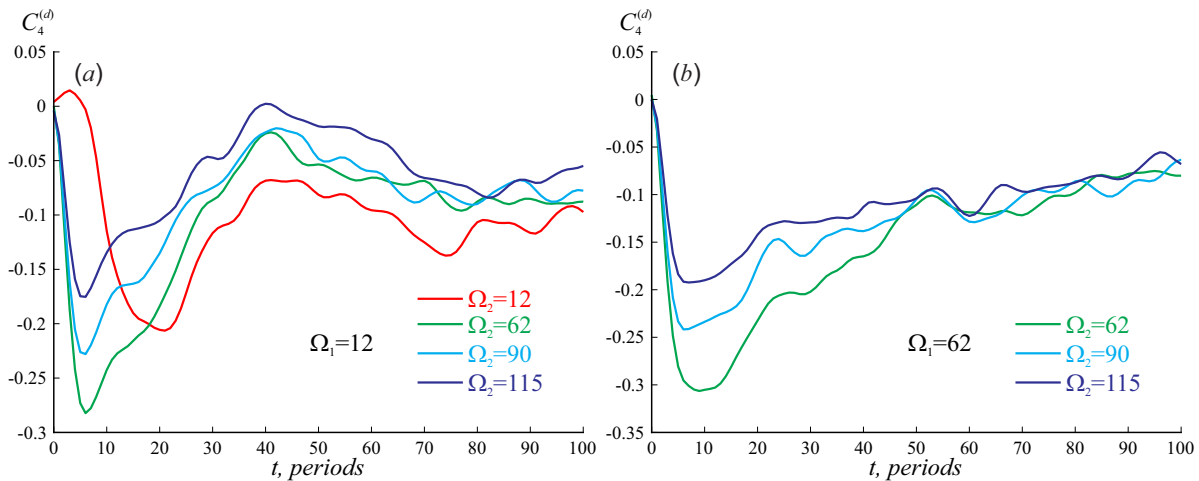


Figure 4: Evolution of the dynamical kurtosis for wave fields with two spectral peaks. Initial conditions are taken as the sum of two JONSWAP spectra. The first spectrum has the same peak frequency ω_p as in figure 1, half of the total energy, $\gamma = 6$ and (a) $\Omega = 12$ (b) $\Omega = 62$. The second spectrum has peak at $1.5\omega_p$ and different directional distribution, as shown in the figure. The total nonlinearity of the combined wave system is the same as in figure 1

3. Long-term evolution of wind wave spectrum and comparison with observations

In this project, we performed preliminary comparisons between the numerical simulations of the evolution of wind-generated waves and observations of fetch-limited waves generated by strong offshore winds in the Gulf of Tehuantepec by Romero & Melville (2010). Both DNS-ZE and KE demonstrate close evolution of integral characteristics of spectra, in good agreement with the experiment. However, the DNS-ZE results show different spectral shapes, considerably wider and with a less pronounced peak than in the simulations obtained with the kinetic equation (figure 7). There is a striking discrepancy between the spectral peak amplitudes, which are, for large times, considerably larger in the case of the kinetic equations than the DNS-ZE prediction. The observed spectra for large times are shown to have the spectral width and the shape of the peak very close to those of the DNS-ZE spectra.

References

- Annenkov, S.Y. & Shrira, V.I. 2013 Large-time evolution of statistical moments of a wind wave field. *J. Fluid Mech.* **726**, 517–546.
- Annenkov, S.Y. & Shrira, V.I. 2014 Evaluation of skewness and kurtosis of wind waves parameterized by JONSWAP spectra. *J. Phys. Oceanogr.* **44**, 1582–1594.
- Annenkov, S.Y. & Shrira, V.I. 2016 Modelling transient sea states with the generalised kinetic equation, In: *Rogue and Shock Waves in Nonlinear Dispersive Media*, M.Onorato et al (eds), Springer.
- Annenkov, S.Y. & Shrira, V.I. 2018 Spectral evolution of weakly nonlinear random waves: kinetic description vs direct numerical simulations, *J. Fluid Mech.* **844**, 766–795.
- Janssen, P.A.E.M. 2009 On some consequences of the canonical transformation in the Hamil-

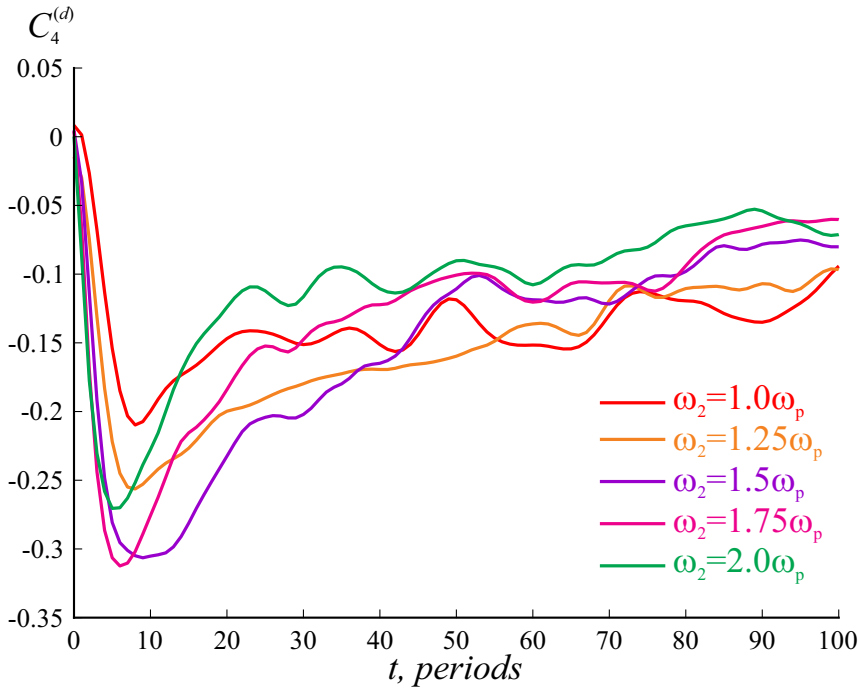


Figure 5: Evolution of the dynamical kurtosis for wave fields with two spectral peaks, as in figure 4b, for $\gamma = 6$ and $\Omega = 62$. The first spectrum has peak frequency ω_p , the second spectrum has spectral peak at various positions between ω_p and $2\omega_p$

tonian theory of water waves. *J. Fluid Mech* **637**, 1–44.

Janssen, P.A.E.M. 2014 On a random time series analysis valid for arbitrary spectral shape. *J. Fluid Mech* **759**, 236–256.

Onorato, M., Cavaleri, L., Fouques, S., Gramstad, O., Janssen, P.A.E.M., Monbaliu, J., Osborne, A.R., Pakozdi, C., Serio, M., Stansberg, C.T. & Toffoli, A. 2009 Statistical properties of mechanically generated surface gravity waves: a laboratory experiment in a three-dimensional wave basin. *J. Fluid Mech.* **627**, 235–257.

Romero, L. & Melville, W.K. 2010 Airborne observations of fetch-limited waves in the Gulf of Tehuantepec. *J. Phys. Oceanogr.* **40**, 441–465.

Toffoli, A., Gramstad, O., Trulsen, K., Monbaliu, J., Bitner-Gregersen, E. & Onorato, M. 2010 Evolution of weakly nonlinear random directional waves: laboratory experiments and numerical simulations. *J. Fluid Mech.* **664**, 313–336.

Xiao, W., Liu, Y., Wu, G. & Yue, D. K. 2013 Rogue wave occurrence and dynamics by direct simulations of nonlinear wave-field evolution. *J. Fluid Mech.* **720**, 357–392.

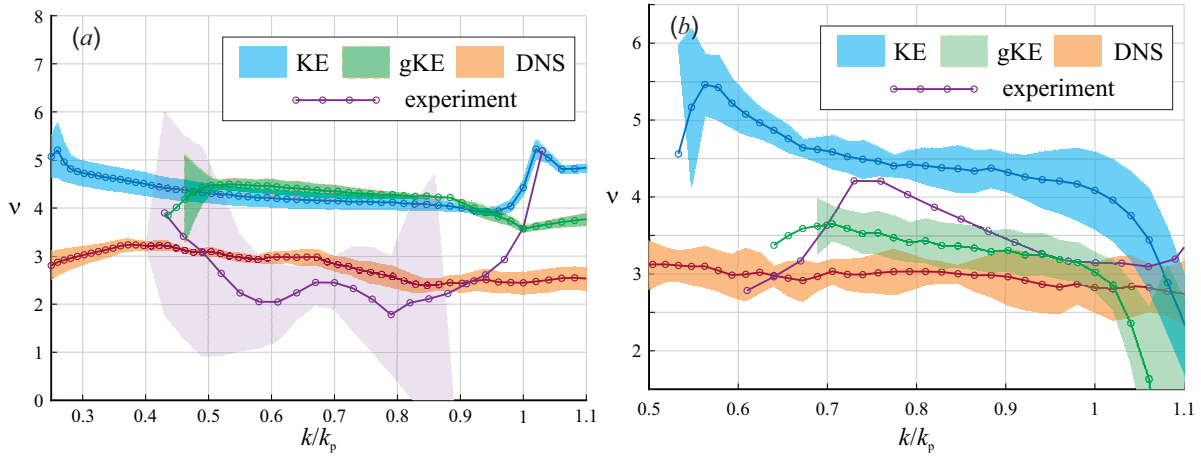


Figure 6: Exponent ν of the scaling of normalised growth rates with nonlinearity for wind waves, obtained by DNS-ZE, two kinetic equations (KE and gKE), and measured in the experiment in the large Marseille-Luminy wind-wave facility (a) constant wind (b) wind increased by 50% during wave evolution. Shaded areas show 95% confidence bounds for the obtained exponent

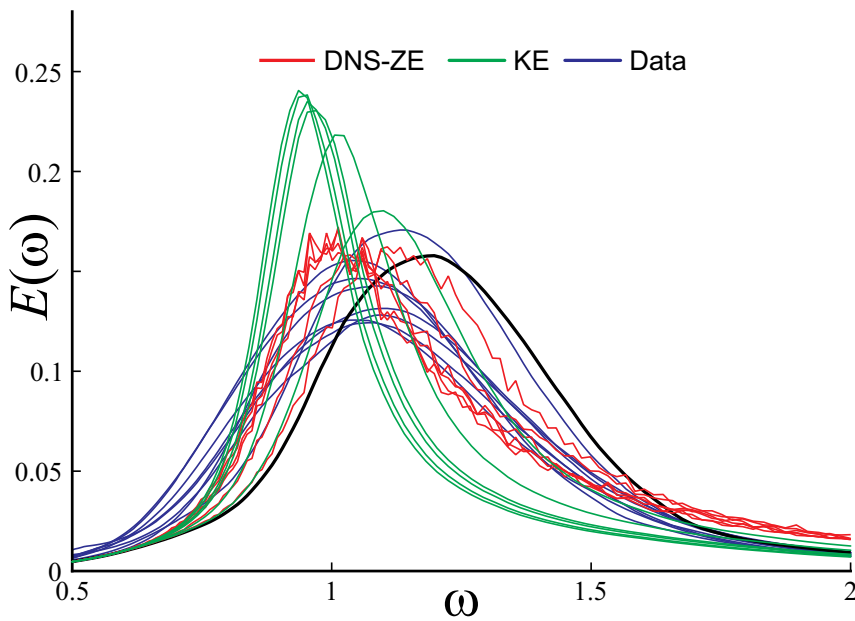


Figure 7: Long-term (over about 400 km of fetch) evolution of energy spectrum measured in the Tehuantepec experiment and modelled by DNS-ZE and the Hasselmann equation

List of publications/reports from the project with complete references

1. Annenkov, S.Y. & Shrira, V.I. 2018 Spectral evolution of weakly nonlinear random waves: kinetic description vs direct numerical simulations. *J. Fluid Mech.* **844**, 766-795.
2. Annenkov, S.Y., Shrira, V.I. & Caulliez, G. 2017 Spectral evolution of weakly nonlinear random waves: kinetic description vs direct numerical simulations and laboratory modelling. IUTAM Symposium on wind waves, 4-8 September 2017, UCL.
3. Annenkov, S.Y., Shrira, V.I. & Caulliez, G. 2018 Evolution of water wave spectra under a sharp increase of wind. Geophysical Research Abstracts Vol. 20, EGU2018-11054.
4. Annenkov, S.Y. & Shrira, V.I. 2018 Long term spectral evolution of wind waves: direct numerical simulations vs kinetic equations modelling and observations. WISE 2018, Tel Aviv University, 22--26 April 2018.

Summary of plans for the continuation of the project

(10 lines max)

In the remaining part of the final year of the project, we will continue the numerical experiments with the dynamical (DNS-ZE) and statistical models, including those based on experimental cases, such as observations of spectral evolution in wind wave tank in Marseille and the Tehuantepec experiment. We will also prepare a number of publications.

.....

.....

.....

.....

.....

.....